Nature and Climate Effects of Individual Tropospheric Aerosol Particles

Mihály Pósfai[1] and Peter R. Buseck[2]

[1]Department of Earth and Environmental Sciences, University of Pannonia, Veszprém, H8200 Hungary; email: posfaim@almos.vein.hu

[2]School of Earth and Space Exploration and Department of Chemistry/Biochemistry, Arizona State University, Tempe, Arizona 85287-1404; email: pbuseck@asu.edu

Annu. Rev. Earth Planet. Sci. 2010. 38:17–43

First published online as a Review in Advance on January 4, 2010

The *Annual Review of Earth and Planetary Sciences* is online at earth.annualreviews.org

This article's doi:
10.1146/annurev.earth.031208.100032

0084-6597/10/0530-0017$20.00

Key Words

atmospheric composition, particle properties, single-particle methods, TEM, electron microscopy

Abstract

Aerosol particles in the atmosphere exert a strong influence on climate by interacting with sunlight and by initiating cloud formation. Because the tropospheric aerosol is a heterogeneous mixture of various particle types, its climate effects can only be fully understood through detailed knowledge of the physical and chemical properties of individual particles. Here we review the results of individual-particle studies that use microscopy-based techniques, emphasizing transmission electron microscopy and focusing on achievements of the past ten years. We discuss the techniques that are best suited for studying distinct particle properties and provide a brief overview of major particle types, their identification, and their sources. The majority of this review is concerned with the optical properties and hygroscopic behavior of aerosol particles; we discuss recent results and highlight the potential of emerging microscopy techniques for analyzing the particle properties that contribute most to climate effects.

INTRODUCTION

GHG: greenhouse gases

RF: radiative forcing

Climate change is strongly affected by both the gaseous and particle components of the atmosphere. Both also profoundly influence quality of life through their effects on health, visibility, and the environment. Although knowledge about gases, including greenhouse gases (GHG), is well advanced, aerosol particles are far less understood. The difference arises in part because of the analytical challenges facing the chemical and physical study of small particles (Buseck & Schwartz 2003). Furthermore, their heterogeneous distribution and shorter atmospheric lifetimes than gases make studying them even more complex. In this review we focus on aerosols, which are composed of particles suspended in a gas—the air, in our case.

Aerosol particles are ubiquitous. They scatter sunlight, thereby reducing the energy flux at the surface of Earth. The result is a cooling effect. Some particles also absorb solar radiation, resulting in a warming of the atmosphere but a cooling of Earth's surface. The interactions of aerosol particles with sunlight result in the direct effect on climate (Yu et al. 2006). Also, several types of indirect effects result from the interactions of particles with clouds and exert a cooling influence. For a cloud with a given water content, an increase in the number of particles results in a proportional increase in droplet number and a decrease in droplet size, producing an increase in cloud albedo (Twomey 1977). Because small droplets are less likely to precipitate than large ones, the lifetime of clouds is extended (Albrecht 1989). Other cloud-mediated effects include changes in precipitation processes and perturbation of the hydrological cycle. This perturbation arises from the production of more upward heat transport for the same amount of surface precipitation (Lohmann & Feichter 2005, Andreae & Rosenfeld 2008). Far greater uncertainties are associated with the indirect aerosol effects than with the direct ones.

A comprehensive summary of current knowledge on aerosol climate effects is the report of the Intergovernmental Panel on Climate Change (IPCC) (Forster et al. 2007). It uses radiative forcing (RF), expressed in W m^{-2}, to describe changes in net irradiance at the tropopause relative to assumed preindustrial values. A positive RF warms the Earth-atmosphere system, and a negative RF cools it. The IPCC report estimates that the RF attributable to human-induced changes in the aerosol burden is between 0 and –3 W m^{-2} (**Figure 1**).

Global warming has been widely known for many years, and its causes from emissions of GHG are relatively well understood as indicated by the large relative probability of their estimated RF (**Figure 1**). The gradual decrease in solar intensity at Earth's surface that occurred for at least several decades in the twentieth century and has been termed global dimming (Wild et al. 2007) is less well known, but it likely resulted at least in part from increases in the atmospheric burden of aerosol particles. Observations of changes in downward shortwave radiation at Earth's surface indicate that the trend has reversed since the 1980s, resulting in global brightening.

One can see striking examples of dimming and brightening caused by the radiative effects of aerosols. Ramanathan et al. (2007) noted a marked drop in sunlight at the surface of the Indian Ocean relative to areas far from the continents and showed that it results from a tenfold increase in airborne soot and other aerosol particles. A pollution layer reduced sunlight by 10%. The many small particles incorporated into clouds increased the reflection of light back into space, turning the clouds into "giant mirrors" and inhibiting a cleansing of the atmosphere through rainout. These results suggest that aerosol particles provide an explanation for dimming.

Our understanding of the influence of aerosol particles on climate change received an unanticipated and unfortunate boost following the destruction of the Twin Towers in New York City on September 11, 2001. All aircraft were immediately grounded over the U.S. for three days, and the lack of aircraft contrails during this short period produced a remarkably strong and rapid response in the weather system. Data across 5000 U.S. weather stations during those few days showed a

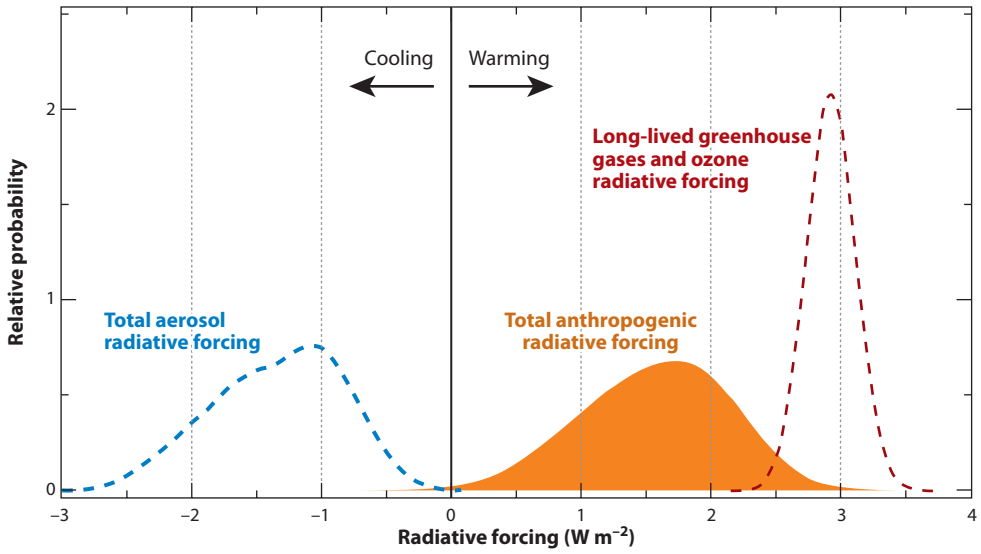

Figure 1

Probability distribution functions of combined anthropogenic radiative forcings (RFs) as estimated by the IPCC. The area under the solid orange curve indicates the sum of all anthropogenic RFs; RFs by greenhouse gases and ozone are represented by the dashed red curve, and aerosol direct and indirect RFs are represented by the dashed blue curve. Surface albedo, contrails, and stratospheric water vapor RFs are included in the total curve but not in the others. Figure from Forster et al. (2007): *Climate Change 2007: The Physical Science Basis. Working Group I Contribution to the Fourth Assessment Report of the Intergovernmental Panel on Climate Change*. Figure 2.20. Cambridge University Press.

dramatic change in the daily temperature range that exceeded the mean over the past 30 years by 1.1°C (e.g., Travis et al. 2002). This incident offered a glimpse of what can be expected in the future if and when the aerosol burden in the atmosphere is reduced.

However, we face a major conundrum: If the concentration of aerosol particles decreases, which would be desirable for the reasons mentioned in the opening paragraph, and if the release of GHG continues—as seems likely—global warming will accelerate. Uncertainties in knowledge about the aerosol RF mean that estimates of climate sensitivity to human perturbations are highly uncertain. If the true aerosol RF lies at the lower end of the range in **Figure 1**, then aerosol RF has protected us from most warming by GHG. Even in a scenario with an aerosol RF between –1 and –1.5 W m^{-2}, our climate will become more sensitive to reductions in the aerosol burden, with the likely consequence that we will face greater warming than current models suggest (Andreae et al. 2005). Thus, there is an urgency to increase knowledge of aerosol RF, which depends, among many other factors, on the physical and chemical properties of aerosol particles.

Individual-particle measurements provide uniquely detailed information on particle properties. The techniques can be grouped into online and offline methods; aerosol mass-spectrometry techniques belong in the former group and microscope-based methods belong in the latter (Buseck & Pósfai 1999, Anastasio & Martin 2001, Buseck et al. 2002, Murphy 2005, Buseck & Adachi 2008). This review focuses on individual particles as seen and understood using microscope techniques. We highlight implications of recent methodological advances in imaging and spectroscopy using various types of microscopes. Then the basic physical and chemical nature of the globally important particle types are discussed, with emphasis on potential future research directions. In the last section we discuss the optical and hygroscopic properties of aerosol particles that have a major

influence on climate. We review recent results of individual-particle studies and identify key areas in which microscope techniques will likely produce important results that will lead to a better understanding of aerosol climate effects in the future.

EDS: energy-dispersive X-ray spectrometry

SEM: scanning electron microscopy

TEM: transmission electron microscopy

MICROSCOPE METHODS FOR THE STUDY OF ATMOSPHERIC PARTICLES

Ideally, we would like to know all the details of the physical and chemical properties of aerosol particles. The main advantage of using microscope methods is that they can provide simultaneous information on several particle properties, but each technique has its special uses and disadvantages (**Table 1**).

Composition

Energy-dispersive X-ray spectrometry (EDS), used with both scanning and transmission electron microscopy (SEM and TEM, respectively), detects characteristic X-ray photons emitted by

Table 1 Applications, strengths, and weaknesses of microscope-based individual-particle methods

Method	Particle properties that can be determined				Advantages and drawbacks
	Size and shape	Composition	Structure	Surface and hygroscopic properties	
SEM	~20 nm resolution with an FEG-SEM; surface shapes from secondary electron images	Element analysis with EDS; semiquantitative for light elements (C, N, O); artifacts in the spectrum	No	ESEM for the study of hydration/dehydration cycles	If automated, can give good statistics; relatively low spatial and compositional specificity; only surface information in images
TEM	Better than 0.1 nm resolution possible; accurate three-dimensional morphology from ET	Element analysis with EDS or EELS; energy-filtered images for element mapping; suitable for light elements in thin (<100 nm) particles	Yes, from electron diffraction	ETEM for the study of hydration/dehydration cycles	High spatial specificity for shape, composition, and structure; can see particle interiors; manually operated and labor-intensive, resulting in poor statistics
STXM	~35 nm for imaging and ~100 nm for spectroscopy; 2D shape with poor resolution	Composition and bonding environment by NEXAFS; element- or bond-specific images	Indirectly from NEXAFS	No	Specific bond types can be studied in carbonaceous aerosol; synchrotron radiation needed; low spatial resolution
AFM	~2 nm resolution; approximate 3D morphology	No	No	Works under ambient conditions; hydration/dehydration cycles can be studied	Mechanical properties of surfaces can be studied; interpretation of results ambiguous; no compositional information

AFM: atomic force microscopy; ED: electron diffraction; EDS: energy-dispersive X-ray spectrometry; EELS: electron energy-loss spectroscopy; ESEM: environmental scanning electron microscopy; ET: electron tomography; ETEM: environmental transmission electron microscopy; FEG: field-emission gun; NEXAFS: near-edge X-ray absorption fine-structure spectroscopy; SEM: scanning electron microscopy; TEM: transmission electron microscopy; STXM: scanning transmission X-ray microscopy.

elements that are excited by an incident electron beam. Simultaneous information can be gathered from a wide range of elements, and the spectra can be used for rapid quantitative analyses (Post & Buseck 1984, Laskin et al. 2005). Electron energy-loss spectrometry (EELS) is based on the detection of electrons that lose energy through inelastic interactions as they are transmitted through the sample. The EELS signal can be used for quantitative analysis of element concentrations (Maynard 1995), and the fine structure of spectra provides information on element bonding and thus structural order (Katrinak et al. 1992). By selecting the signal from electrons having specific energies, EELS can also be used to create maps of element distributions in a particle, and chemical inhomogeneities can be visualized within complex particles (Pósfai & Molnár 2000, Pósfai et al. 2003b, Hand et al. 2005). Scanning transmission X-ray microscopy (STXM) coupled with near-edge X-ray absorption fine-structure spectroscopy (NEXAFS), done using a synchrotron, has recently seen use in atmospheric science. The technique is similar to EELS but has greater energy and poorer spatial resolution. It is particularly useful for the analysis of carbonaceous particles because the compositions of organic functional groups can be inferred from the bonding state of C (Russell et al. 2002, Tivanski et al. 2007) and S (Hopkins et al. 2008).

EELS: electron energy-loss spectrometry

STXM: scanning transmission X-ray microscopy

NEXAFS: near-edge X-ray absorption fine-structure spectroscopy

ET: electron tomography

AFM: atomic force microscopy

SAED: selected-area electron diffraction

ESEM: environmental scanning electron microscopy

ETEM: environmental transmission electron microscopy

Size and Morphology

The most obvious function of any microscope technique is obtaining pictures, and the most evident particle properties one can extract from these are size and shape. Several operationally defined particle sizes are used in atmospheric science (Johnston et al. 2006), and it is not generally obvious which agrees best with the diameters measured in microscopes. Images are usually two-dimensional (2D) projections, so information on the third dimension of the particle is lost. However, three-dimensional (3D) particle morphologies can be determined using electron tomography (ET) and atomic force microscopy (AFM). ET involves the acquisition of a series of TEM images, obtained at regular intervals of sample tilt angles (e.g., 2°) relative to the electron beam. This series is then used for a 3D reconstruction of particle morphology. ET can provide unique high-resolution information on the shapes of particles (van Poppel et al. 2005, Adachi et al. 2007). AFM complements other types of analyses (Barkay et al. 2005, Gwaze et al. 2007), but the lack of direct compositional information and the artifacts arising from the interactions between the cantilever tip and specimen have limited AFM use in atmospheric science.

Structure

Whether tropospheric aerosol particles are crystalline or amorphous is generally considered to be of secondary importance in atmospheric studies. However, crystallinity is important in many ways. The ice nucleation activity of particles depends strongly on their structures, as do the optical properties of absorbing materials such as some carbonaceous particles. Selected-area electron diffraction (SAED) with TEM is the method of choice when direct structural information is needed from individual particles (Pósfai et al. 1995, Li et al. 2003b). SAED is useful for identifying structures and, indirectly, aerosol particles for which the compositional data are ambiguous.

Hygroscopicity and Surface Reactions

Sample chambers that allow gas introduction have recently been developed for SEM and TEM. The techniques (sometimes also the instruments) are termed ESEM and ETEM, respectively, because of the environmental chamber. ESEM has been used for visualizing and measuring the hygroscopic growth of individual particles (Ebert et al. 2002a, Hiranuma et al. 2008), studying

heterogeneous surface reactions (Krueger et al. 2003, Hoffman et al. 2004, Laskin et al. 2005), and studying the ice nucleation capability of particles (Zimmermann et al. 2007). ETEM has emerged as a powerful technique for measuring the hygroscopic growth and deliquescence of particles at a much higher resolution than is possible with ESEM (Wise et al. 2005, 2007; Semeniuk et al. 2007a,b; Freney et al. 2009). The method is uniquely useful for understanding the hygroscopic behavior of complex, internally mixed aerosol particles. AFM was used in a few cases for measuring the hygroscopic behavior of atmospheric aerosol particles (Pósfai et al. 1998, Köllensperger et al. 1999, Ramirez-Aguilar et al. 1999) and studying surface reactions (Zangmeister & Pemberton 2000).

Mixing States

The mixing state of an aerosol particle indicates whether distinct, homogeneous entities occur within the same particle (internally mixed, such as an aggregate of different phases) or whether they are separated in the air (externally mixed). Any of the methods mentioned above can be used to determine mixing states as long as the resolution of the technique is suitable for observing intraparticle heterogeneities. Knowledge of mixing states is crucial for modeling studies and can be used to infer the hygroscopic (Okada et al. 2005) or optical properties (Pósfai et al. 1999) of particles and to provide information about their atmospheric histories (aging and reactions) (Li et al. 2003a,b; Pósfai et al. 2003b) and sources (Niemi et al. 2004, 2006).

MAJOR PARTICLE TYPES: IDENTIFICATION, ABUNDANCES, COMPOSITIONS, AND SOURCES

Apart from special cases such as some mineral dust or industrial pollution close to the emission source, particles formed by different processes occur as internal mixtures in the atmosphere (Murphy et al. 2006). Therefore, any classification of particles based on either composition or source is somewhat arbitrary, and overlaps between the groups are unavoidable. Here we distinguish sulfate, sea-salt, mineral-dust, and carbonaceous particles. The carbonaceous particles are further divided into primary biogenic, combustion-produced, and secondary organic groups. The source strength and atmospheric burden of each particle group are estimated in several reviews (e.g., Forster et al. 2007, Andreae & Rosenfeld 2008) and summarized in **Table 2**. In this section we discuss the results and potential of individual-particle microscope studies for the identification of specific particle types, their abundances, and their sources.

Table 2 Estimated emissions and atmospheric burdens of the major particles types (based on Andreae & Rosenfeld 2008 and references therein)

	Mass emission (Tg year^{-1})		
	Minimum	Maximum	Mass burden (Tg)
Sulfates	107	374	2.8
Nitrates	12	27	0.49
Sea salt	3000	20,000	15
Mineral dust	1000	2150	18 ± 5
Industrial dust	40	130	1.1
Biogenic primary organic	15	70	0.2
Biomass burning organic	26	70	–
Black carbon (soot)	8	14	0.1
Secondary organic	2.5	83	0.8

Sulfates

Sulfate particles, whose compositions range from sulfuric acid to ammonium sulfate, constitute a major aerosol type in the troposphere—and probably are the best known. They either nucleate homogeneously or form on existing particles from gaseous precursors of both natural—i.e., marine dimethylsulfide (DMS)—and anthropogenic (SO_2) origins, with the anthropogenic fraction dominating. Anthropogenic SO_2 emissions decreased by ~25% between 1980 and 2000, with the major emitting regions shifting from Europe and North America to Southeast Asia (Liu et al. 2005).

DMS: dimethylsulfide

The S isotopic composition of sulfate particles depends on both the source of the precursor SO_2 and the homogeneous or heterogeneous oxidation processes that led to sulfate formation, and thus can shed light on origin. Winterholler et al. (2008) combined secondary ion mass spectrometry at the nanoscale (NanoSIMS) with SEM/EDS for the analysis of urban aerosol particles. All secondary sulfate particles were isotopically homogeneous, suggesting cloud processing. Owing to the different oxidation states of S in methanesulfonate (a product of biogenic DMS oxidation) and in sulfate, the ratios of these two species could be determined in individual sea-salt particles by fitting empirical curves to the S L-edge in NEXAFS spectra obtained using STXM (Hopkins et al. 2008). Methanesulfonate salts were the dominant form of non-sea-salt sulfur in large particles, and sulfate appeared to be more common in smaller particles.

Sea Salt

In terms of mass, sea-salt particles are second only to mineral dust in abundance in the troposphere (Andreae & Rosenfeld 2008). They arise through the bursting of bubbles that rise to the sea surface (Blanchard & Woodcock 1957), and their size distributions, reactions, and optical and cloud nucleating effects are well known (O'Dowd et al. 1997, Murphy et al. 1998, Lewis & Schwartz 2004). Their size distributions are bimodal: one mode at 2.5 μm corresponds to particles produced by jet drops, and another mode at ~0.1 μm corresponds to particles produced by film drops (Mårtensson et al. 2003). Individual-particle mass spectrometry showed that sea-salt particles contain ~10% organic matter (Middlebrook et al. 1998). The surface microlayer of the ocean is enriched in microorganisms, viruses, and extracellular biogenic material (Aller et al. 2005), all of which can enter the atmosphere through bubble bursting. However, it is unknown whether these biogenic constituents are internally mixed with sea salt (**Figure 2**) or whether they also form a significant pool of externally mixed organic particles, as suggested by Bigg & Leck (2008). Despite both bulk studies (O'Dowd et al. 2004) and morphological and indirect chemical observations of individual particles (Leck & Bigg 2005), the nature of particles smaller than ~200 nm in the marine atmosphere needs to be clarified.

Mineral Dust

Most mineral dust in the troposphere originates from the dust belt, a chain of arid regions that includes the Sahara and the deserts in the Middle East and China. Dried lakebeds and other once-wet areas are particularly important sources of atmospheric dust (Prospero 1999). Desert dust can be the dominant particle type even thousands of kilometers from the source. In addition to its direct and indirect climate effects, atmospheric dust plays an important role in the global biogeochemical cycle of iron, a limiting nutrient in many oceanic ecosystems (Jickells et al. 2005).

Particle reactions and internal mixing during transport of mineral dust can substantially change the composition of the original aerosol. Even relatively close to the source, calcite and halite

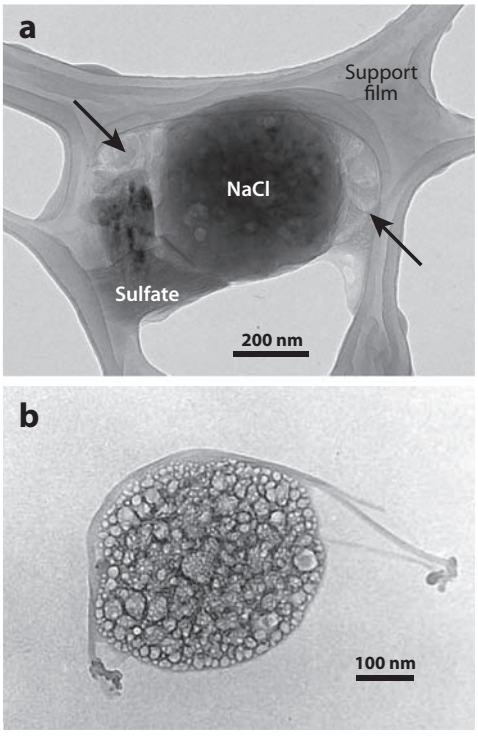

Figure 2

Electron micrographs of particles from the marine atmosphere. (*a*) Sea-salt particle that consists of a NaCl crystal, mixed-cation sulfate, and filamentous organic material, presumably of primary marine origin (*marked by arrows*). (*b*) A sulfate particle from the North Atlantic, with a carbonaceous filament. The mottled texture results from decomposition of ammonium sulfate in the electron beam.

partially reacted to sulfate in a dust storm in the Taklamakan Desert (Okada & Kai 2004). In certain desert areas, dust types that contained a significant fraction of carbonate minerals acted as effective sinks for nitric acid (Krueger et al. 2004). Carbonate minerals can also convert to sulfate (Sobanska et al. 2003) or both sulfate and nitrate (Matsuki et al. 2005). Mineral particles become internally mixed with sea salt, perhaps through cloud processing (Niimura et al. 1998, Trochkine et al. 2003). Saharan minerals were associated with sulfur and organic matter from both urban and agricultural pollution in Israel (Falkovich et al. 2001) and with organics from combustion above the Pacific (Gao et al. 2007), suggesting that mineral dust is a potential cleansing agent for organic pollutants. Understanding the stimulation of phytoplankton growth by iron-bearing atmospheric dust requires detailed knowledge of the mineralogy of the aerosol (Cwiertny et al. 2008).

Primary Biogenic Particles

Primary biogenic particles in the atmosphere include (in size sequence) living and dead viruses, bacterial cells, spores, pollen, and biogenic debris such as marine colloids and plant fragments (**Figure 3**). The number concentrations of biogenic particles range from minor fractions of the total aerosol in oceanic (1%) (Pósfai et al. 2003a) and continental (2 to 3%) settings (Winiwarter et al. 2009), to ~25% in a continental aerosol (Matthias-Maser & Jaenicke 1994) and 35% in Amazonia (Elbert et al. 2007). This range reflects the variability of sources and particle types.

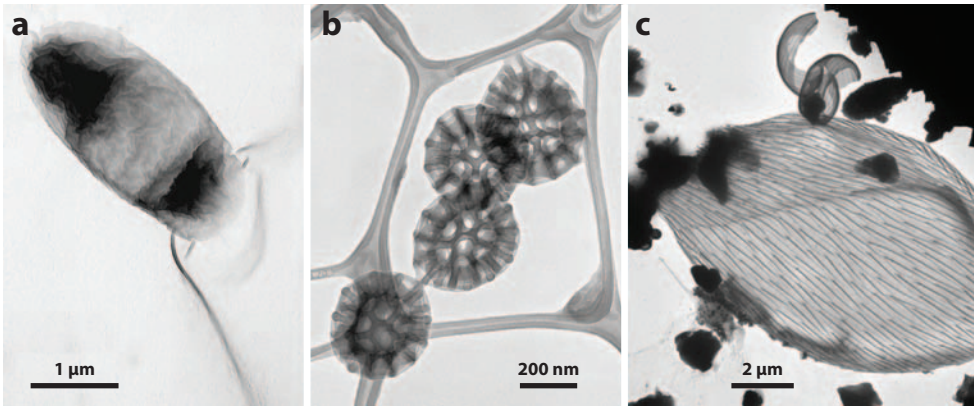

Figure 3

Electron micrographs of biogenic particles. (*a*) An unidentified marine microorganism from the Southern Ocean atmosphere. (*b*) Brochosomes (C-, O-, and Si-bearing particles secreted by leaf-hopping insects) from Southern Africa. (*c*) Biogenic debris, probably plant fragments, collected at a rural site in Hungary.

Various methods of collection and analysis are used for the study of bioaerosols; the most useful results on the types and concentrations of microorganisms come from studies that combine microscopy with cultivation (Bauer et al. 2002).

Many problems in atmospheric science are related to primary biological particles, including the spread of pathogens and the roles of microorganisms in cloud and ice nucleation (Morris et al. 2008). There are indications that some bacteria show metabolic activity in cloud droplets (Sattler et al. 2001). If the activity of microorganisms in the atmosphere is confirmed by further studies, new pathways of aerosol and cloud-droplet chemistry will have to be considered.

Methods adopted from molecular environmental biology provide unique data on airborne organisms (Maron et al. 2005) and were used to assess the diversity of biological material (Després et al. 2007). Although such methods offer insight into the ensemble makeup of the aerosol, genetic information on individual particles may be available in the future if organism-specific fluorescent probes are constructed and combined with microscopy. The use of modern biological methods triggered a revolutionary change in the solid earth sciences and led to the development of new fields such as geomicrobiology. A similar explosion of research involving the study of individual bioaerosol particles is likely in atmospheric science.

Combustion-Derived Carbonaceous Particles

Soot is the most studied and best-known particle type produced by the combustion of fossil fuels, residential biofuel, and biomass. The atmospheric science community commonly uses the terms black carbon (BC) for the strongly absorbing component of the aerosol and elemental carbon (EC) for the most refractory part of the carbonaceous aerosol that oxidizes above a certain threshold in combustion experiments. However, as pointed out by Bond & Bergstrom (2006) and Andreae & Gelencsér (2006), BC and EC are ill-defined terms, and in the following we avoid their use. Instead, we define soot as a primary, combustion-produced particle type that has a distinctive structure consisting of graphene-like layers that are wrapped into spherules tens of nanometers in diameter and that resemble nano-onions. The spherules aggregate into branching or compact clusters.

HRTEM: high-resolution transmission electron microscopy

The characteristic layered structure of soot spherules, which can be observed using high-resolution TEM (HRTEM), is diagnostic for soot identification in complex, internally mixed

Figure 4

HRTEM image of the nanostructure of soot showing wavy, graphene-like layers wrapped into spherules.

particles (Pósfai et al. 1999) (**Figure 4**). The nanostructural features of soot particles reflect their distinct sources (including oil boilers, jet aircraft, and diesel engines) (Hays & Vander Wal 2007). In addition to the structures of primary spherules, the fractal properties of soot aggregates are influenced by fuel type and combustion conditions. In some cases a source apportionment was possible from the structure variations and fractal parameters of atmospheric soot (Wentzel et al. 2003, van Poppel et al. 2005).

Although the controlled technological burning of fossil fuels emits almost pure soot, a much greater variety of carbonaceous particles results from biofuel, agricultural, and uncontrolled biomass fires (Reid et al. 2005). Biomass burning produces atmospheric particles in amounts that affect both the regional and global climate (Forster et al. 2007). In the past ten years individual-particle TEM studies greatly advanced our understanding of particles from biomass fires and revealed that agricultural fires severely affect atmospheric composition and air quality, even in developed regions such as Europe (Niemi et al. 2004, 2006) and North America (Hudson et al. 2004). In addition to soot, the major particle types include organic particles, many of which contain inorganic salt inclusions (Martins et al. 1998, Li et al. 2003b, Pósfai et al. 2003b).

A new and distinctive particle type was identified from biomass-burning emissions; it was given the name tar ball (Pósfai et al. 2003b, 2004). Although spherical, tar balls are larger than individual soot spherules and lack their graphitic structures. They mainly consist of C and O, and can contain N and traces of S, Si, and other elements. Although the distribution of C is homogeneous, O is enriched in the ~30-nm outer layer of the spherules (Hand et al. 2005). Their organic compositions resemble those of atmospheric humic-like substances (Tivanski et al. 2007).

SOA: secondary organic aerosol

VOC: volatile organic compound

Secondary Organic Aerosol

The formation and effects of secondary organic aerosol (SOA) particles are among the most studied aspects of current aerosol science. They form from volatile organic compounds (VOCs) that are

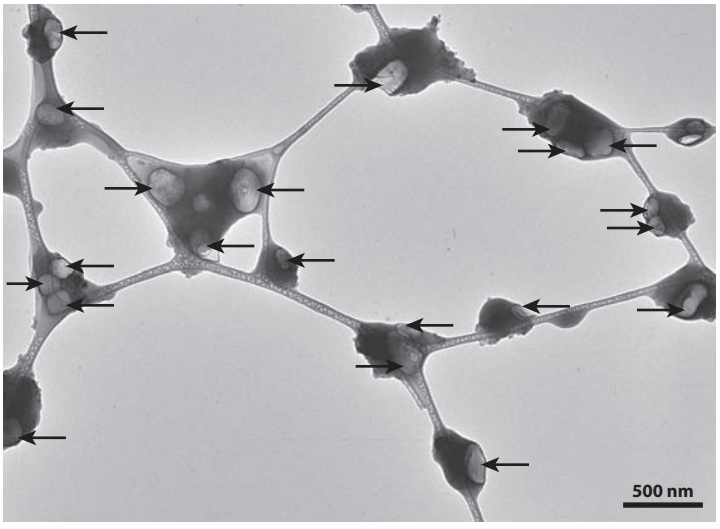

Figure 5

Electron micrograph of organic/sulfate mixed particles from the continental troposphere. The arrows mark voids where the sulfate component of the particles was volatilized by the electron beam. The thin fibers are from the lacey-carbon substrate.

emitted by both biogenic and anthropogenic sources, with the biogenic contribution believed to be globally dominant (Tsigaridis & Kanakidou 2007). Isoprene and terpene emitted by terrestrial plants are likely the most important natural sources (Claeys et al. 2004), and combustion produces anthropogenic precursors. Photooxidation of VOCs reduces their vapor pressure, and organic gases condense onto existing aerosol particles. Polymerization continues in the condensed phase and results in semi- or nonvolatile organic species (Gelencsér 2004). Estimates of the global strengths of various SOA sources vary widely (Andreae & Rosenfeld 2008), reflecting the need for more detailed studies on this class of particles.

Individual-particle studies using both mass spectrometry (Murphy et al. 2006) and electron microscopy (Pósfai & Molnár 2000) have shown a wide range of S/C ratios in particles from clean and polluted regions. A significant fraction likely consists of SOA/sulfate mixtures (**Figure 5**). The nucleation of nanometer-sized sulfate particles was observed in rural, urban, and coastal environments (Kulmala et al. 2004). Laboratory studies show that sulfate nucleation is enhanced by aromatic acids (Zhang et al. 2004); thus, organics are already present in some sulfate particles at nucleation. Because of further condensation of organics onto the freshly nucleated particles, SOA/sulfate mixed particles result (Adachi & Buseck 2008, Smith et al. 2008). SOA particles are amorphous and composed of light elements, so of the major particle types they are the least amenable to study using methods such as conventional TEM and SEM. Combinations of spectroscopic and microscope methods (e.g., TEM/EELS or STXM/NEXAFS) seem the most promising for studying the structures and compositions of individual SOA particles.

PARTICLE PROPERTIES AND THEIR EFFECTS ON CLIMATE

The optical properties of aerosol particles affect their direct RF of climate. Light scattering and absorption by particles are determined by their sizes, complex refractive indices, and morphologies, properties that are rather inhomogeneous in space and time (Seinfeld & Pandis 2006). Whereas light scattering, absorption, and extinction by a bulk aerosol can be obtained using ground-based,

RH: relative humidity

CCN: cloud condensation nuclei

airborne, or satellite measurements, no straightforward experimental method is available to assess the contributions of distinct particle types to these quantities. To estimate the direct RF of the aerosol, we need to know the sizes, morphologies, and scattering and absorption cross sections (α_{sca} and α_{abs}, respectively) for each particle type. Because α_{sca} and α_{abs} depend on the complex refractive index, which, in turn, is a function of the composition and structure, individual-particle microscope methods can be used to provide data from which indirect information about optical properties can be obtained. Even more importantly, in the atmosphere particles are typically mixed with other species that result in a wide and unknown range of scattering and absorption efficiencies. Uncertainties about the degree and nature of internal mixing among particle types can be reduced by single-particle observations. Below we discuss the results of some individual-particle studies that advanced our knowledge about the optical properties of aerosol types, particularly those of carbonaceous matter, including both black and brown carbon.

The hygroscopic behavior of aerosol particles also has important consequences for both their direct and indirect climate effects. At relative humidities (RHs) under 100%, the uptake of water makes certain particles grow, thereby changing their scattering and absorption cross sections; particles in the 0.5- to 2-μm range are the most efficient light scatterers. Condensation of water can also make small particles grow into the size range in which they become activated as cloud condensation nuclei (CCN), thereby modifying the radiative properties and lifetimes of clouds (Lohmann & Feichter 2005). In addition to the radiative and cloud effects related to changes in particle sizes, the aerosol water provides a medium for aqueous-phase chemical reactions that can alter the chemistry and morphology of particles.

The hygroscopic behavior of homogeneous, inorganic particles such as many salts is well known. In contrast, the hygroscopic properties of organic particles and particularly of complex mixtures of inorganic and organic species are just beginning to be understood. The hygroscopic properties can be inferred from the analysis of compositions and structures of individual particles. The advent of the aforementioned ESEM and ETEM techniques ushered in an exciting new era of research because they allow us to study the hygroscopic behavior of particles directly.

Particle Morphology and its Effects on Scattering and Absorption

Scattering and absorption by spherical particles can be computed using conventional Mie theory. Some aerosol types, including sulfates, commonly occur in liquid droplets and can safely be considered spherical. However, soot, mineral particles, microorganisms, and many other aerosol types have nonspherical shapes that can strongly affect their optical properties (Mishchenko et al. 2000).

Soot is the strongest absorber of solar radiation among all major atmospheric particle types. Because soot absorbs shortwave radiation and reemits the absorbed energy as heat, it produces a strong positive RF (Jacobson 2002). Soot can play a role in cloud formation, resulting in brown clouds with enhanced absorption of solar radiation and consequently producing a semidirect RF (Ramanathan & Carmichael 2008). Thus, the climate effects of soot have many aspects, all related to its optical properties. However, the values of key parameters needed to understand the scattering and absorption by soot, including particle size and complex refractive index, vary widely in the literature (Bond & Bergstrom 2006).

Soot particles are agglomerates of primary spherules. Both scattering and absorption are affected by their complex particle morphologies (Fuller et al. 1999). If a particle is an aggregate of same-sized spherules, it can be characterized as a mass fractal. Scattering and absorption by aggregates can be calculated using the Rayleigh-Debye-Gans (RDG) approximation (Sorensen 2001), for which both the fractal parameters and complex refractive index must be known. The fractal parameters of atmospheric soot have been estimated from 2D projections in TEM, AFM,

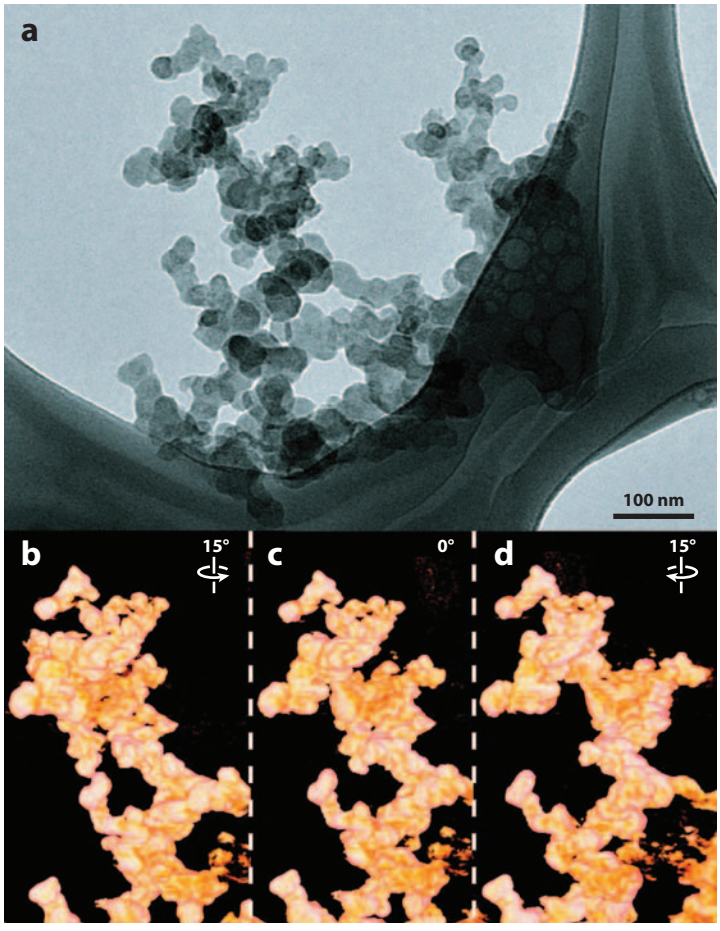

Figure 6

Two-dimensional TEM image of soot versus 3D electron tomography (ET) images. (*a*) TEM image of a soot particle collected above Mexico City. ET images of the same soot particle: (*b*) rotated 15° counterclockwise around the vertical axis, (*c*) with the same orientation as the TEM image in (*a*), and (*d*) rotated 15° clockwise around the vertical axis. Image courtesy of Kouji Adachi, ASU.

and SEM images (Katrinak et al. 1993, Wentzel et al. 2003, Gwaze et al. 2007, Smekens et al. 2007). However, recent work shows that fractal parameters derived from 2D images can be highly inaccurate.

ET can be used to obtain 3D reconstructions of the particles, from which more accurate data can be obtained (van Poppel et al. 2005, Adachi et al. 2007). Overlapping parts and holes cannot be distinguished in the conventional bright-field image in **Figure 6*a***, but a 3D reconstruction allows viewing and measuring the particle along any direction, resulting in an accurate evaluation of its fractal parameters. **Figure 6** shows three projections (parts *b*, *c*, and *d*) of the 3D reconstruction of the central part of the particle in **Figure 6*a***. Even though the viewing direction differs by only 15°, the particle looks very different depending on orientation; for example, it appears to be much more compact in **Figure 6*b*** than in **Figure 6*d***.

Using ET, Adachi et al. (2007) measured fractal parameters for soot particles from Asian dust and from traffic sources. The values were used for calculations based on the RDG theory. Albeit

Table 3 Examples of optical parameters in the wavelength range of 500 to 550 nm of various absorbing carbonaceous aerosol species

	Refractive index	Mass scattering cross section ($m^2\ g^{-1}$)	Mass absorption cross section ($m^2\ g^{-1}$)	References
Fresh soot	$1.95 + 0.79i$	1.4 to 2.0	7.5 ± 1.2	Adachi et al. 2007; Bond & Bergstrom 2006; Andreae & Gelencsér 2006
Humic-like substances (HULIS)	$1.67 + 0.017i$	2.25	0.03	Hoffer et al. 2006; Andreae & Gelencsér 2006
Tar ball	$1.67 - 0.27i$	3.2 to 3.7	3.6 to 4.1	Alexander et al. 2008

for a small sample, the most interesting results are that mass-normalized scattering cross section (σ_{sca}) values derived for the soot aggregate particles were 20 to 28 times those for unaggregated spherical particles of the same mass. A 15% enhancement was found for the mass-normalized absorption cross section (σ_{abs}) values of aggregates versus unaggregated spheres (**Table 3**). The greater enhancement of scattering than absorption means that aggregates have a larger single-scattering albedo than separated spheres.

Modeling studies generally assume spherical soot particles and thus may seriously underestimate their scattering. Because lognormal size distributions that include large spheres are typically used in models, the scattering by large particles may offset the error caused by the assumption of spherical shapes (Adachi et al. 2007). Further ET studies on fresh and aged soot particles as well as those with and without coatings will provide the models with input parameters that are superior to the input parameters currently in use.

Although not normally as complex as those of soot, mineral particles can have a variety of shapes. Their sharp edges and angular features result in differences in the scattering phase function, asymmetry parameter, optical depth, and single scattering albedo relative to those of the volume-equivalent spheres that are commonly assumed (Kalashnikova & Sokolik 2002). Approximate shapes derived from microscope images were used in model calculations, and different mineral groups appeared to be best approximated using different geometric forms such as disk shapes for clay particles and ellipsoids for quartz, calcite, and dolomite particles (Hudson et al. 2008). Because the shapes of mineral particles can also depend on their sources and weathering, it will remain difficult to properly account for shape-dependent optical properties of dust particles.

Complex Refractive Index

The effects of the material properties on the optical behavior of a particle are manifested in the complex refractive index, which is generally given as $m = n + ki$, where $i = -1^{1/2}$. Scattering is mainly a function of n; absorption is primarily determined by the imaginary part, although it is also affected by the real part of m. Experimental approaches for obtaining more accurate refractive indices include either measurement of the optical properties of pure substances (which can be either extracts from real aerosol samples or surrogates for ambient aerosol types), or study of the structure and composition of the particles from which the refractive index can be inferred (Ebert et al. 2002b, 2004; Kandler et al. 2007; Alexander et al. 2008). Although the refractive indices of inorganic salts and minerals are well known and given in textbooks, obtaining the refractive indices of the highly variable atmospheric carbonaceous particles remains a major challenge.

The absorption of light by carbonaceous particles is related to their structure, in particular the fraction of sp^2-type bonds (i.e., covalent bonds as in a graphene layer, with the bonding electrons in sp^2 hybrid orbitals). The imaginary part of the refractive index of soot, as well as other

carbonaceous particle types, is determined by the fraction and size of the graphite-like, aromatic structural elements. Soot also contains sp^3-type bonds, consistent with its content of elements other than C (primarily H). For ambient carbonaceous particles with absorptive properties that range from those of diesel soot to those of organic particles (Bond & Bergstrom 2006, Kirchstetter & Novakov 2007), the analysis of either structure or bond type can lead to an estimate of the refractive index.

HULIS: humic-like substances

UV: ultraviolet

The structure of soot can be directly visualized in HRTEM images (Li et al. 2003b, Wentzel et al. 2003). Palotas et al. (1996) used Fourier transforms of such images to analyze interplanar spacings, circularity, orientation, elongation, and length distribution of lattice fringes in various types of soot. Kis et al. (2006) derived quantitative data on atomic distances from the radial intensity distribution in SAED patterns of soot emitted by savanna burning and residential heating. They found smaller values for nearest-neighbor distances than in graphite or amorphous carbon, which suggests that the soot contains abundant H-bearing aromatic rings. The graphene-like structures probably exist as small clusters of a few rings within the layers of the soot spherules. Because interatomic distances provide information on bond types, in principle quantitative electron diffraction could be used to derive complex refractive indices for carbonaceous particle types.

The carbon bond type is reflected in certain features in Raman, electron energy-loss, and X-ray absorption spectra. Whereas Raman spectroscopy can be used to obtain the sp^2 bond fraction in bulk samples (Sze et al. 2001), EELS and STXM/NEXAFS are applicable to individual particles. By using the intensity ratios within specific energy windows in NEXAFS spectra, researchers evaluated the percentage of sp^2 hybridization in individual particles (Hopkins et al. 2007, Takahama et al. 2007). The sp^2 hybridization values are 100% for highly ordered pyrolitic graphite, and they range from 41% to 69% for black carbon reference materials. Atmospheric soot particles range from 29% to 82%, which suggests that their complex refractive indices vary widely.

Mounting evidence suggests that brown carbon is a significant component of the tropospheric aerosol (Andreae & Gelencsér 2006). Some brown carbon species form during combustion, and others may be SOA particles that form in the air from volatile precursors in photochemical reactions. Attempts have been made to obtain refractive indices for reasonably well-defined organic particle types that may qualify as brown carbon and for ensembles of carbonaceous particles such as those that form during biomass burning (Kirchstetter et al. 2004). Tar balls were identified using individual-particle TEM studies (Pósfai et al. 2004). Their complex refractive indices were calculated from dielectric functions that were measured from EELS spectra (Alexander et al. 2008) (**Table 3**), and confirm that they are brown. Atmospheric humic-like substances (HULIS) were defined on the basis of their ensemble chemistry, molecular mass, and spectral properties (Gelencsér 2004). The optical properties of HULIS were determined on re-aerosolized material that was chemically isolated from biomass-burning aerosol (Hoffer et al. 2006). A common property of brown carbon species is a strong wavelength dependence of their absorption (Kirchstetter et al. 2004, Hoffer et al. 2006). Both tar balls and HULIS absorb light effectively at ~300 nm wavelength. The absorption of downward ultraviolet (UV) radiation by atmospheric brown carbon may turn out to be a globally important component of direct RF.

Mixing States and Optical Properties

It follows from the above that size, morphology, and refractive index are affected by whether aerosol species having different material properties exist in the air as separate particles or as internally mixed particles. The most significant changes in optical properties produced by internal mixing are caused by the formation of particles that consist of both absorbing and nonabsorbing (or weakly absorbing) components such as water, sulfate, or organic material.

DRH: deliquescence relative humidity

ERH: efflorescence relative humidity

A large fraction of soot occurs internally mixed with sulfates or secondary organic species in both urban (Adachi & Buseck 2008, Schwarz et al. 2008) and remote environments (Pósfai et al. 1999). Model calculations show that the absorption of soot is enhanced by a nonabsorbing coating, and the degree of enhancement depends on the geometrical relationship between core and coating (Fuller et al. 1999). An enhancement factor of ~2 over externally mixed particles results if a soot core is encapsulated in a nonabsorbing sulfate or organic shell. Laboratory experiments with soot particles that were artificially coated with organic material show good agreement with calculations, producing absorption amplification factors between 1.8 and 2.1 (Schnaiter et al. 2005). The large variation in mixing ratios may be the cause of the wide range of observed mass absorption cross sections (from 6 to 20 $m^2\ g^{-1}$) (Liousse et al. 1993).

Climate models that calculate the direct RF by aerosol particles need to use assumptions about how to treat the effects of internal mixing of soot with other species. For example, Jacobson (2001) included coagulation and particle growth processes in his model, which resulted in coated soot particles that produced positive forcing (~0.55 $W\ m^{-2}$) sufficient to nearly balance the cooling effect of other anthropogenic aerosol particles. The most recent IPCC report deduced a direct RF of $+0.20 \pm 0.15\ W\ m^{-2}$ by averaging many model results (Forster et al. 2007), and Ramanathan & Carmichael (2008) calculated a range between 0.4 and 1.2 $W\ m^{-2}$. The results illustrate how much uncertainty remains in the assessment of the radiative effects of soot, especially in relation to its mixing properties.

Hygroscopic Behavior Under 100% Relative Humidity

Size changes resulting from hygroscopic effects are a major influence on the direct RF by aerosol particles in the troposphere (Wang et al. 2008). Two groups of particles can be distinguished based on their hygroscopic properties: those that deliquesce and those that do not. Inorganic salts typically show deliquescent behavior, which means that they form liquid droplets as they dissolve at a material-specific deliquescence relative humidity (DRH). Upon decreasing RH, such particles crystallize at an efflorescence relative humidity (ERH). The ERH is much lower than the DRH, resulting in a hysteresis effect. Although deliquescent particles have a thin water layer on their surfaces even when crystalline, they do not grow significantly by water adsorption below the DRH. In contrast, other particles (e.g., H_2SO_4) grow monotonically with increasing RH and do not show deliquescence or efflorescence. The hygroscopic behavior, including the exact DRH and ERH values of most atmospherically relevant inorganic salts, is well established (Martin 2000). However, the hygroscopic growth of complex mixtures of inorganic and organic matter in ambient particles is difficult to predict from the properties of their individual constituents.

In the past few years ESEM and ETEM measurements greatly increased knowledge of the hygroscopic behavior of individual particles between 0% and 100% RH. The first ESEM (Ebert et al. 2002a) and ETEM (Wise et al. 2005) studies showed that DRH and ERH values can be determined and that solid and liquid particles can be distinguished during full cycles of deliquescence and efflorescence (**Figure 7**). In the first ETEM study of complex internal mixtures, Wise et al. (2007) studied NaCl-bearing particles. The DRH value of sea-salt particles containing sulfates was slightly lower than that for pure NaCl (74% instead of 76%). Interestingly, $NaNO_3$-bearing sea-salt particles showed morphological changes between 40% and 65% RH. ESEM measurements by Hoffman et al. (2004) also found that $NaNO_3$ in sea-salt aerosol exhibits continuous hygroscopic growth. $NaNO_3$-bearing sea-salt particles deliquesced at 70%, a value lower than the DRHs for pure $NaNO_3$ (74.3%) and NaCl (76%) (Wise et al. 2007). These individual-particle results are consistent with the well-known observation that the DRH of a mixed salt is lower than the DRHs of its individual components (Seinfeld & Pandis 2006).

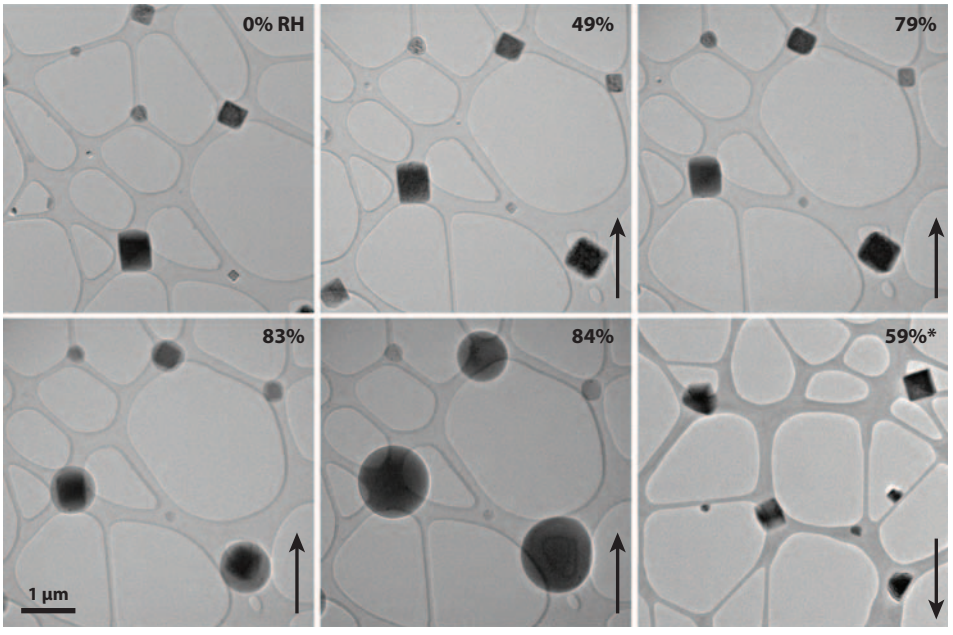

Figure 7

Atomized KCl particles deposited onto a TEM grid and exposed to changing relative humidity (RH). The arrows indicate whether the RH was being increased (*up arrow*) or decreased (*down arrow*). Predeliquescent water uptake can be seen on the particles at an RH of 83%. Deliquescence occurred at an RH of 84%. Efflorescence occurred at an RH of 59%. Asterisk indicates that the image is of a different field of view. Image courtesy of Evelyn Freney, ASU. The thin fibers are from the lacey-carbon substrate.

Nitrates cause significant changes in the hygroscopic growth of mineral particles. Grains coated with $Ca(NO_3)_2$ retained water even at 15% RH, whereas the morphologies of bare and sulfate-containing mineral particles did not change between 15% and 90% RH (Shi et al. 2008). If calcite reacts to form nitrate, it becomes highly hygroscopic (Laskin et al. 2005). The high resolution of ETEM allowed the detailed observation of multistep deliquescence of aggregated or coated particles (Semeniuk et al. 2007b). Their hygroscopic behavior reflected their heterogeneous makeup because the constituents with the lowest DRH (such as NaCl) first started to accrue water, whereas the rest of the particle did not show changes.

Studies of the hygroscopic behavior of mixed organic/inorganic particles using electrodynamic balances, particle mobility analyzers, and infrared absorption cells show that the deliquescence and efflorescence behavior of such mixed particles cannot be predicted from the properties of their individual components. For example, organic acids in mixed particles reduced the water absorption of NaCl but enhanced that of $(NH_4)_2SO_4$ (Cruz & Pandis 2000, Choi & Chan 2002). Malonic and citric acid caused the inorganic salts to absorb a significant amount of water before deliquescence, whereas glutaric acid caused them to deliquesce gradually, spanning a wide range of RH (Choi & Chan 2002). In general, if the organic fraction is significant in mixed organic/$(NH_4)_2SO_4$ particles, the ERH is lower than that of pure sulfate and the particles will likely remain liquid (Pant et al. 2004).

Hiranuma et al. (2008) used ESEM to study a rural aerosol consisting mostly of carbonaceous particles. Although it was not possible to simultaneously study the composition and hygroscopic behavior of these particles, most exhibited low water uptake up to 96% RH and did not show

deliquescence. Similar behavior was shown by some pyrogenic particles from biomass burning in Southern Africa, with soot and tar-ball particles showing no water uptake up to 100% RH (Semeniuk et al. 2007a). Interestingly, aged tar balls collected in North America appeared to take up some water at ~83% RH in an ESEM (Hand et al. 2005). The apparent contradiction between these two studies could result either from the aging of the tar balls, which caused compositional changes that made them hygroscopic, or from an insufficient resolution of ESEM that may not have allowed the distinction of tar balls from other organic particles.

In biomass-burning aerosol from South Africa, organic particles containing inorganic salt inclusions took up water between 55% and 100% RH in an ETEM study (Semeniuk et al. 2007a). In many cases the inorganic phase inside or attached to the particle showed deliquescence, whereas most of the particle volume remained unchanged. Thus, the inorganic components appeared to dramatically affect the hygroscopic behavior of the predominantly organic particles and determined the RH at which water uptake started.

An interesting ETEM observation on marine aerosol indicated water uptake at 56% RH in a splatter zone around sea-salt particles. The phenomenon was taken as evidence for the presence of water-soluble, hygroscopic organics associated with sea salt (Wise et al. 2007). These ETEM studies demonstrate that the deliquescence and efflorescence of particles can now be observed at formerly unprecedented spatial resolution, but that the behavior with water is more complex than is commonly assumed.

Particle Types That Can Form Cloud Condensation Nuclei

The fundamentals of cloud-droplet activation can be found in textbooks and reviews (e.g., Andreae & Rosenfeld 2008). Cloud-droplet nucleation is governed by the Kelvin and Raoult effects. Because the equilibrium vapor pressure over a strongly curved surface is larger than over a flat surface (Kelvin effect), the homogeneous nucleation of water droplets requires enormous supersaturations. Therefore, cloud droplets form by heterogeneous nucleation on particles that have large enough radii of curvature to oppose the Kelvin effect. Moreover, water molecules condense preferentially on water-soluble particles because the equilibrium vapor pressure over a solution is lower than that over pure water (Raoult effect). As described by classical Köhler theory, for each soluble particle size there is a critical supersaturation, S_c, at which point the droplet spontaneously grows.

At each supersaturation value (typically from 0.1% to 1%), CCN are a subset of all aerosol particles that can be activated to form cloud droplets. According to observed CCN spectra (ratios of CCN versus all particles as a function of particle size at a given supersaturation), aerosols that consist of entirely soluble particles such as sulfate or sea salt are much more efficient CCN than those dominated by hydrophobic particles (e.g., pyrogenic aerosol) (Andreae & Rosenfeld 2008). The compositions and activation of individual particles can be directly observed using the novel techniques of ESEM and ETEM. Examples are discussed below for mineral and organic aerosol particles.

When a hydrophobic particle such as a mineral grain is coated by a small amount of soluble material, S_c can be reduced drastically (Levin et al. 2005). Indeed, mineral particles were observed by TEM to be aggregated with sulfate, sea salt, and other soluble species and interpreted as having been cloud-processed (Wurzler et al. 2000, Kojima et al. 2006). Because of their large sizes and soluble contents, these modified particles can serve as giant CCN and thus have a significant impact on cloud development. Giant CCN greatly influence cloud albedo by decreasing the Twomey effect (Feingold et al. 1999). A direct approach was used to study the CCN activity of mineral dust that reacted with nitrogen oxides (Gibson et al. 2007). The CCN activity of a $CaCO_3$-$Ca(NO_3)_2$ aerosol was significantly enhanced relative to $CaCO_3$ particles

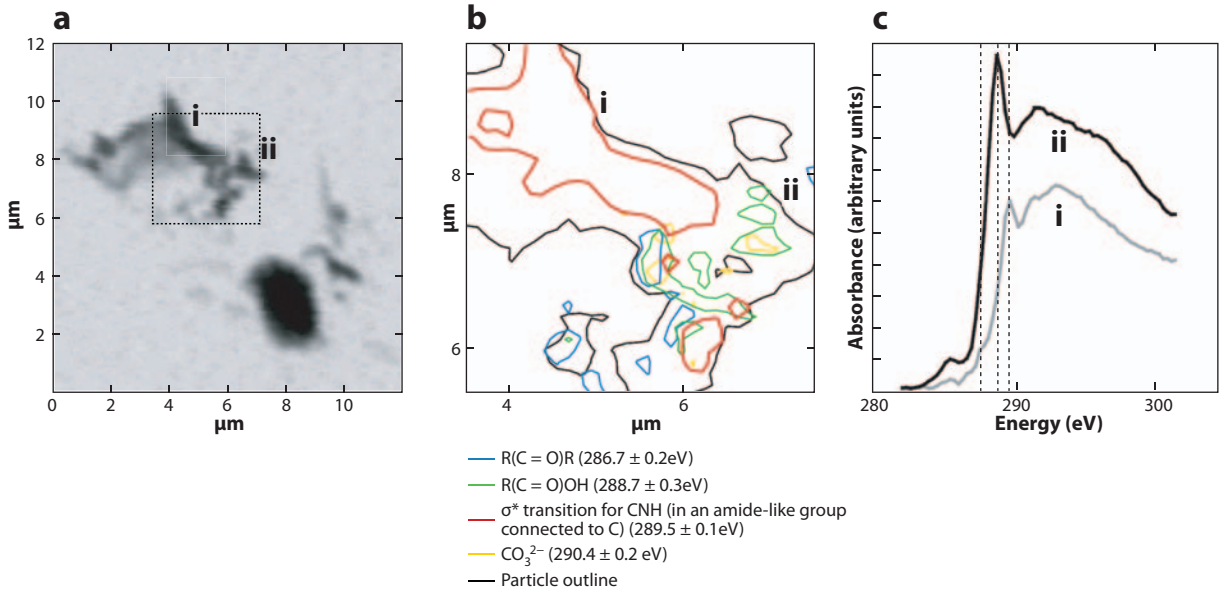

Figure 8

(*a*) STXM absorbance image at 300.0 eV, (*b*) chemical contour map of the boxed area in (*a*), and (*c*) NEXAFS spectra of the particles marked *i* and *ii* in (*a*). The particles were collected in the marine boundary layer. Threshold contours (*b*) at the detection limits are drawn in different colors for different functional groups. Image courtesy of Lynn Russell, based on figure 1 in Russell et al. (2002).

of the same diameter. Similar results were obtained for kaolinite that was internally mixed with $(NH_4)_2SO_4$.

Köhler theory was developed for soluble inorganic salts, so it fails to adequately describe the effects of organic compounds that either partially or gradually dissolve. Also, surface-active organic material can reduce the surface tension or form hydrophobic surface films, both of which can cause major changes in the Kelvin term and change the CCN activity of the particle (Kiss et al. 2005). Even small amounts of soluble inorganic material can change a slightly soluble organic particle into a CCN (Bilde & Svenningsson 2004). The study of the hygroscopic behavior of organic matter in aerosol particles and cloud droplets and their effects on CCN activity is reviewed by Gelencsér (2004) and Sun & Ariya (2006).

Using spectral windows with STXM/NEXAFS that are specific to various carbon bonds, Russell et al. (2002) mapped the distribution of alkyl, ketonic carbonyl [R(C = O)R], carboxylic carbonyl [R(C = O)OH], and alkene groups within particles collected in the marine atmosphere of the Caribbean (**Figure 8**). The coatings of these particles contain an elevated proportion of the more oxygenated carboxylic carbonyl groups that likely affect the condensation and evaporation of water. Another individual-particle study on cloud residue particles used TEM/EELS to show that N-bearing organic particles act as CCN even without containing soluble inorganic material (Twohy et al. 2005).

Particle Types That Can Form Ice Nuclei

Aerosol particles that induce the formation of ice particles are named ice nuclei (IN). Whereas homogeneous freezing of water occurs at –36 to –38°C, heterogeneous nucleation of ice can occur at temperatures up to –1°C (Vali 1985). Ice particles in clouds are a major factor in developing

IN: ice nuclei

precipitation and shaping the radiative properties of clouds (Cantrell & Heymsfield 2005). Because the vapor pressure of ice is lower than that of water, ice particles grow faster than water droplets and thus will initiate precipitation. Intriguingly, an inverse aerosol indirect effect was observed over the Indian Ocean, where the IN activity of polluted aerosol resulted in almost a doubling of ice-crystal sizes in cirrus clouds. The consequence was that such clouds reflected less sunlight and let more thermal radiation escape into space (Chylek et al. 2006).

The number of IN in the atmosphere is low; typically fewer than one in a million particles are active (Andreae & Rosenfeld 2008). IN-active aerosol particles are identified either in laboratory ice-nucleation experiments or by the analysis of ice-cloud residues. Studies of cirrus ice residues found many types of IN, including mineral dust, meteoritic material, metals (DeMott et al. 2003), $(NH_4)_2SO_4$ (Cziczo & Abbatt 1999, Kojima et al. 2005), soot (Twohy & Gandrud 1998), and bacteria (Möhler et al. 2007). Mineral-dust particles appear to be particularly common IN. Interestingly, their activity does not seem to depend on the particular dust source (Field et al. 2006).

The field results for the IN activity of organic aerosol appear contradictory, presumably reflecting the variable character of organic particles. An SEM/EDS study of the residues of orographic clouds containing pollution aerosol showed IN-active mineral dust and metallic particles, whereas clean air masses of oceanic origin contained low-Z, probable organic material that inhibited ice formation (Targino et al. 2006). Cziczo et al. (2004) also observed that organic material remained unfrozen in cirrus clouds. In contrast, oxalic acid dihydrate crystals acted as IN; this finding was based on laboratory ice-nucleation studies and observations by single-particle mass spectrometry of relatively large concentrations of oxalic acid in upper tropospheric clouds. In general, the relative importance of the different types of IN in the various environments of atmospheric ice formation remains largely unknown. As indicated by a pilot ESEM study of ice nucleation on silver iodide, kaolinite, and montmorillonite (Zimmermann et al. 2007), the emerging techniques of ESEM and ETEM will likely become valuable tools for obtaining data on the composition and structure-specific IN activities of individual particles.

SUMMARY

Atmospheric aerosol particles have important consequences for climate, environment, and health. Microscope imaging and chemical analyses are extremely useful for determining multiple physical and chemical properties for given individual particles, thereby providing unique data that can be used for the assessment of aerosol climate effects. Moreover, through their visual appeal, microscope images instill new ideas in atmospheric chemists and modelers and influence the field even beyond the significance of the quantitative data that can be extracted from them. In this review we highlighted the most important results of microscope-based aerosol studies of the past ten years and brought attention to emerging techniques. Various combinations of new imaging and spectroscopy techniques reveal the molecular and structural makeup of aerosol species at formerly unprecedented spatial resolution, whereas environmental electron microscopy permits the in situ observation of the hygroscopic behavior of individual particles. These techniques are particularly useful for obtaining new knowledge about the optical properties and the cloud- and ice-nucleation activities of the major particle types. The goal is that this new knowledge will inform modeling studies and lead to a significantly improved understanding of aerosol climate effects.

DISCLOSURE STATEMENT

The authors are not aware of any affiliations, memberships, funding, or financial holdings that might be perceived as affecting the objectivity of this review.

ACKNOWLEDGMENTS

We thank Drs. Kouji Adachi and Evelyn Freney, both at ASU, for critical comments on portions of the manuscript and for use of their TEM images. We thank Dr. Lynn Russell for use of **Figure 8**. We thank Dr. Ágnes Molnár for a critical reading of the entire manuscript. This study was supported by a grant from the Hungarian Science Fund (OTKA-49845) and the Atmospheric Chemistry Division of the National Science Foundation under grant number ATM-0531926.

LITERATURE CITED

Adachi K, Buseck PR. 2008. Internally mixed soot, sulfates, and organic matter in aerosol particles from Mexico City. *Atmos. Chem. Phys.* 8:6469–81

Adachi K, Chung SH, Friedrich H, Buseck PR. 2007. Fractal parameters of individual soot particles determined using electron tomography: implications for optical properties. *J. Geophys. Res.* 112:D14202

Albrecht B. 1989. Aerosols, cloud microphysics and fractional cloudiness. *Science* 245:1227–30

Alexander DTL, Crozier PA, Anderson JR. 2008. Brown carbon spheres in East Asian outflow and their optical properties. *Science* 321:833–36

Aller JY, Kuznetsova MR, Jahns CJ, Kemp PF. 2005. The sea surface microlayer as a source of viral and bacterial enrichment in marine aerosols. *J. Aerosol Sci.* 36:801–12

Anastasio C, Martin ST. 2001. Atmospheric nanoparticles. *Rev. Mineral. Geochem.* 44:293–349

Andreae MO, Gelencsér A. 2006. Black carbon or brown carbon? The nature of light-absorbing carbonaceous aerosols. *Atmos. Chem. Phys.* 6:3131–48

Andreae MO, Jones CD, Cox PM. 2005. Strong present-day aerosol cooling implies a hot future. *Nature* 435:1187–90

Andreae MO, Rosenfeld D. 2008. Aerosol-cloud-precipitation interactions. Part 1. The nature and sources of cloud-active aerosols. *Earth-Sci. Rev.* 89:13–41

Barkay Z, Teller A, Ganor E, Levin Z, Shapira Y. 2005. Atomic force and scanning electron microscopy of atmospheric particles. *Microsc. Res. Tech.* 68:107–14

Bauer H, Kasper-Giebl A, Loflund M, Giebl H, Hitzenberger R, et al. 2002. The contribution of bacteria and fungal spores to the organic carbon content of cloud water, precipitation and aerosols. *Atmos. Res.* 64:109–19

Bigg EK, Leck C. 2008. The composition of fragments of bubbles bursting at the ocean surface. *J. Geophys. Res.* 113:D11209

Bilde M, Svenningsson B. 2004. CCN activation of slightly soluble organics: the importance of small amounts of inorganic salt and particle phase. *Tellus* 56:128–34

Blanchard DC, Woodcock AH. 1957. Bubble formation and modification in the sea and its meteorological significance. *Tellus* 9:145–58

Bond TC, Bergstrom RW. 2006. Light absorption by carbonaceous particles: an investigative review. *Aerosol Sci. Technol.* 40:1–41

Buseck PR, Adachi K. 2008. Nanoparticles in the atmosphere. *Elements* 4:389–94

Buseck PR, Jacob DJ, Pósfai M, Li J, Anderson JR. 2002. Minerals in the air: an environmental perspective. In *Frontiers in Geochemistry: Global Inorganic Geochemistry*, ed. WG Ernst, pp. 106–22. Columbia, MD: Geol. Soc. Am., Bellwether Publ.

Buseck PR, Pósfai M. 1999. Airborne minerals and related aerosol particles: effects on climate and the environment. *Proc. Natl. Acad. Sci. USA* 96:3372–79

Buseck PR, Schwartz SE. 2003. Tropospheric aerosols. In *Treatise on Geochemistry*, ed. KK Turekian, HD Holland, pp. 91–142. New York: Elsevier Science Ltd.

Cantrell W, Heymsfield A. 2005. Production of ice in tropospheric clouds: a review. *Bull. Am. Meteorol. Soc.* 86:795–807

Choi MY, Chan CK. 2002. The effects of organic species on the hygroscopic behaviors of inorganic aerosols. *Environ. Sci. Technol.* 36:2422–28

Chylek P, Dubey MK, Lohmann U, Ramanathan V, Kaufman YJ, et al. 2006. Aerosol indirect effect over the Indian Ocean. *Geophys. Res. Lett.* 33:L06806, doi:10.1029/2005GL025397

Claeys M, Graham B, Vas G, Wang W, Vermeylen R, et al. 2004. Formation of secondary organic aerosols through photooxidation of isoprene. *Science* 303:1173–76

Cruz CN, Pandis SN. 2000. Deliquescence and hygroscopic growth of mixed inorganic–organic atmospheric aerosol. *Environ. Sci. Technol.* 34:4313–19

Cwiertny DM, Baltrusaitis J, Hunter GJ, Laskin A, Scherer MM, Grassian VH. 2008. Characterization and acid-mobilization study of iron-containing mineral dust source materials. *J. Geophys. Res.* 113:D05202, doi:10.1029/2007JD009332

Cziczo DJ, Abbatt JPD. 1999. Deliquescence, efflorescence, and supercooling of ammonium sulfate aerosols at low temperature: implications for cirrus cloud formation and aerosol phase in the atmosphere. *J. Geophys. Res.* 104:13781–90

Cziczo DJ, DeMott PJ, Brooks SD, Prenni AJ, Thomson DS, et al. 2004. Observations of organic species and atmospheric ice formation. *Geophys. Res. Lett.* 31:L12116, doi:10.1029/2004GL019822

DeMott PJ, Cziczo DJ, Prenni AJ, Murphy DM, Kreidenweis SM, et al. 2003. Measurements of the concentration and composition of nuclei for cirrus formation. *Proc. Natl. Acad. Sci. USA* 100:14655–60

Després V, Nowoisky J, Klose M, Conrad R, Andreae MO, Pöschl U. 2007. Characterization of primary biogenic aerosol particles in urban, rural, and high-alpine air by DNA sequence and restriction fragment analysis of ribosomal RNA genes. *Biogeosciences* 4:1127–41

Ebert M, Inerle-Hof M, Weinbruch S. 2002a. Environmental scanning electron microscopy as a new technique to determine the hygroscopic behaviour of individual aerosol particles. *Atmos. Environ.* 36:5909–16

Ebert M, Weinbruch S, Hoffmann P, Ortner HM. 2004. The chemical composition and complex refractive index of rural and urban influenced aerosols determined by individual particle analysis. *Atmos. Environ.* 38:6531–45

Ebert M, Weinbruch S, Rausch A, Gorzawski G, Hoffmann P, et al. 2002b. Complex refractive index of aerosols during LACE 98 as derived from the analysis of individual particles. *J. Geophys. Res.* 107(D21):8121, doi:10.1029/2000JD000195

Elbert W, Taylor PE, Andreae MO, Pöschl U. 2007. Contribution of fungi to primary biogenic aerosols in the atmosphere: wet and dry discharged spores, carbohydrates, and inorganic ions. *Atmos. Chem. Phys.* 7:4569–88

Falkovich AH, Ganor E, Levin Z, Formenti P, Rudich Y. 2001. Chemical and mineralogical analysis of individual mineral dust particles. *J. Geophys. Res.* 106:18029–36

Feingold G, Cotton WR, Kreidenweis SM, Davis JT. 1999. The impact of giant cloud condensation nuclei on drizzle formation in stratocumulus: implications for cloud radiative properties. *J. Atmos. Sci.* 56:4100–17

Field PR, Möhler O, Connolly P, Krämer M, Cotton R, et al. 2006. Some ice nucleation characteristics of Asian and Saharan desert dust. *Atmos. Chem. Phys. Discuss.* 6:1509–37

Forster P, Ramaswamy V, Artaxo P, Berntsen T, Betts R, et al. 2007. Changes in atmospheric constituents and radiative forcing. In *Climate Change 2007: The Physical Science Basis. Contribution of Working Group I to the Fourth Assessment Report of the Intergovernmental Panel on Climate Change*, ed. S Solomon, D Qin, M Manning, Z Chen, M Marquis, et al., pp. 129–234. Cambridge, UK, and New York: Cambridge Univ. Press

Freney EJ, Martin ST, Buseck PR. 2009. Deliquescence and efflorescence of potassium salts relevant to biomass-burning aerosol particles. *Aerosol Sci. Technol.* 43:799–807

Fuller KA, Malm WC, Kreidenweis SM. 1999. Effects of mixing on extinction by carbonaceous particles. *J. Geophys. Res.* 104(D13):15941–54

Gao Y, Anderson JR, Hua X. 2007. Dust characteristics over the North Pacific observed through shipboard measurements during the ACE-Asia experiment. *Atmos. Environ.* 41:7907–22

Gelencsér A. 2004. *Carbonaceous Aerosol*. Berlin, Heidelberg, New York: Springer. 350 pp.

Gibson ER, Gierlus KM, Hudson PK, Grassian VH. 2007. Generation of internally mixed insoluble and soluble aerosol particles to investigate the impact of atmospheric aging and heterogeneous processing on the CCN activity of mineral dust aerosol. *Aerosol Sci. Technol.* 41:914–24

Gwaze P, Annegarn HJ, Huth J, Helas G. 2007. Comparison of particle sizes determined with impactor, AFM and SEM. *Atmos. Res.* 86:93–104

Hand JL, Malm WC, Laskin A, Day D, Lee T, et al. 2005. Optical, physical, and chemical properties of tar balls observed during the Yosemite Aerosol Characterization Study. *J. Geophys. Res.* 110:D21210, doi:10.1029/2004JD005728

Hays MD, Vander Wal RL. 2007. Heterogeneous soot nanostructure in atmospheric and combustion source aerosols. *Energy Fuels* 21:801–11

Hiranuma N, Brooks SD, Auvermann BW, Littleton R. 2008. Using environmental scanning electron microscopy to determine the hygroscopic properties of agricultural aerosols. *Atmos. Environ.* 42:1983–94

Hoffer A, Gelencsér A, Guyon P, Kiss G, Schmid O, et al. 2006. Optical properties of humic-like substances (HULIS) in biomass-burning aerosols. *Atmos. Chem. Phys.* 6:3563–70

Hoffman RC, Laskin A, Finlayson-Pitts BJ. 2004. Sodium nitrate particles: physical and chemical properties during hydration and dehydration, and implications for aged sea salt aerosols. *J. Aerosol. Sci.* 35:869–87

Hopkins RJ, Desyaterik Y, Tivanski AV, Zaveri RA, Berkowitz CM, et al. 2008. Chemical speciation of sulfur in marine cloud droplets and particles: analysis of individual particles from the marine boundary layer over the California current. *J. Geophys. Res.* 113:D04209, doi:10.1029/2007JD008954

Hopkins RJ, Tivanski AV, Marten BD, Gilles MK. 2007. Chemical bonding and structure of black carbon reference materials and individual carbonaceous atmospheric aerosols. *J. Aerosol. Sci.* 38:573–91

Hudson PK, Murphy DM, Cziczo DJ, Thomson DS, de Gouw JA, et al. 2004. Biomass-burning particle measurements: characteristics composition and chemical processing. *J. Geophys. Res.* 109:1–11

Hudson PK, Young MA, Kleiber PD, Grassian VH. 2008. Coupled infrared extinction spectra and size distribution measurements for several non-clay components of mineral dust aerosol (quartz, calcite, and dolomite). *Atmos. Environ.* 42:5991–99

Jacobson MZ. 2001. Strong radiative heating due to the mixing state of black carbon in atmospheric aerosols. *Nature* 409:695–97

Jacobson MZ. 2002. Control of fossil-fuel particulate black carbon and organic matter, possibly the most effective method of slowing global warming. *J. Geophys. Res.* 107:4410, doi:10.1029/2001JD001376

Jickells TD, An ZS, Andersen KK, Baker AR, Bergametti C, et al. 2005. Global iron connections between desert dust, ocean biogeochemistry, and climate. *Science* 308:67–71

Johnston MV, Wang S, Reinard MS. 2006. Nanoparticle mass spectrometry: pushing the limit of single particle analysis. *Appl. Spectrosc.* 60:A264–72

Kalashnikova OV, Sokolik IN. 2002. Importance of shapes and compositions of wind-blown dust particles for remote sensing at solar wavelengths. *Geophys. Res. Lett.* 29(10):1398, doi:10.1029/2002GL014947

Kandler K, Benker N, Bundke U, Cuevas E, Ebert M, et al. 2007. Chemical composition and complex refractive index of Saharan Mineral Dust at Izana, Tenerife (Spain) derived by electron microscopy. *Atmos. Environ.* 41:8058–74

Katrinak KA, Rez P, Buseck PR. 1992. Structural variations in individual carbonaceous particles from an urban aerosol. *Environ. Sci. Technol.* 26:1967–76

Katrinak KA, Rez P, Perkes PR, Buseck PR. 1993. Fractal geometry of carbonaceous aggregates from an urban aerosol. *Environ. Sci. Technol.* 27:539–47

Kirchstetter TW, Novakov T. 2007. Controlled generation of black carbon particles from a diffusion flame and applications in evaluating black carbon measurement methods. *Atmos. Environ.* 41:1874–88

Kirchstetter TW, Novakov T, Hobbs PV. 2004. Evidence that the spectral dependence of light absorption by aerosols is affected by organic carbon. *J. Geophys. Res.* 109:D21208, doi:10.1029/2004JD004999

Kis VK, Pósfai M, Lábár JL. 2006. Nanostructure of atmospheric soot particles. *Atmos. Environ.* 40:5533–42

Kiss G, Tombácz E, Hansson H-C. 2005. Surface tension effects of humic-like substances in the aqueous extract of tropospheric fine aerosol. *J. Atmos. Chem.* 50:279–94

Kojima T, Buseck PR, Iwasaka Y, Matsuki A, Trochkine D. 2006. Sulfate-coated dust particles in the free troposphere over Japan. *Atmos. Res.* 82:698–708

Kojima T, Buseck PR, Reeves JM. 2005. Aerosol particles from tropical convective systems: 2. Cloud bases. *J. Geophys. Res.* 110:1–12

Köllensperger G, Friedbacher G, Kotzick R, Niessner R, Grasserbauer M. 1999. In-situ atomic force microscopy investigation of aerosols exposed to different humidities. *Fresenius J. Anal. Chem.* 364:296–304

Krueger BJ, Grassian VH, Cowin JP, Laskin A. 2004. Heterogeneous chemistry of individual mineral dust particles from different dust source regions: the importance of particle mineralogy. *Atmos. Environ.* 38:6253–61

Krueger BJ, Grassian VH, Iedema MJ, Cowin JP, Laskin A. 2003. Probing heterogeneous chemistry of individual atmospheric particles using scanning electron microscopy and energy-dispersive X-ray analysis. *Anal. Chem.* 75:5170–79

Kulmala M, Vehkamäki H, Petäjä T, Dal Maso M, Lauri A, et al. 2004. Formation and growth rates of ultrafine atmospheric particles: a review of observations. *J. Aerosol. Sci.* 35:143–76

Laskin A, Wietsma TW, Krueger BJ, Grassian VH. 2005. Heterogeneous chemistry of individual mineral dust particles with nitric acid: a combined CCSEM/EDX, ESEM, and ICP-MS study. *J. Geophys. Res.* 110:1–15

Leck C, Bigg EK. 2005. Source and evolution of the marine aerosol—a new perspective. *Geophys. Res. Lett.* 32:1–4

Levin Z, Teller A, Ganor E, Yin Y. 2005. On the interactions of mineral dust, sea-salt particles, and clouds: a measurement and modeling study from the Mediterranean Israeli Dust Experiment campaign. *J. Geophys. Res.* 110:D20202, doi:10.1029/2005JD005810

Lewis ER, Schwartz SE. 2004. *Sea Salt Aerosol Production: Mechanisms, Methods, Measurements, and Models: A Critical Review*. Washington, D.C.: Am. Geophys. Union. 413 pp.

Li J, Anderson JR, Buseck PR. 2003a. TEM study of aerosol particles from clean and polluted marine boundary layers over the North Atlantic. *J. Geophys. Res.* 108(D6):4189, doi:10.1029/2002JD002106

Li J, Pósfai M, Hobbs PV, Buseck PR. 2003b. Individual aerosol particles from biomass burning in southern Africa: 2. Compositions and aging of inorganic particles. *J. Geophys. Res.* 108(D13):8484, doi:10.1029/2002JD002310

Liousse C, Cachier C, Jennings SG. 1993. Optical and thermal measurements of black carbon aerosol content in different environments: variation of the specific attenuation cross-section, sigma (σ). *Atmos. Environ.* 27:1203–11

Liu X, Penner JE, Herzog M. 2005. Global modeling of aerosol dynamics: model description, evaluation, and interactions between sulfate and nonsulfate aerosols. *J. Geophys. Res.* 110:1–37

Lohmann U, Feichter H. 2005. Global indirect aerosol effects: a review. *Atmos. Chem. Phys.* 5:715–37

Maron P-A, Lejon DPH, Carvalho E, Bizet K, Lemanceau P, et al. 2005. Assessing genetic structure and diversity of airborne bacterial communities by DNA fingerprinting and 16S rDNA clone library. *Atmos. Environ.* 39:3687–95

Mårtensson EM, Nilsson ED, de Leeuw G, Cohen LH, Hansson H-C. 2003. Laboratory simulations and parameterization of the primary marine aerosol production. *J. Geophys. Res.* 108(D9):4297, doi:10.1029/2002JD002263

Martin ST. 2000. Phase transitions of aqueous atmospheric particles. *Chem. Rev.* 100:3403–53

Martins JV, Hobbs PV, Weiss RE, Artaxo P. 1998. Sphericity and morphology of smoke particles from biomass burning in Brazil. *J. Geophys. Res.* 103:32051–57

Matsuki A, Iwasaka Y, Shi G, Zhang D, Trochkine D, et al. 2005. Morphological and chemical modification of mineral dust: observational insight into the heterogeneous uptake of acidic gases. *Geophys. Res. Lett.* 32:L22806, doi:10.1029/2005GL024176

Matthias-Maser S, Jaenicke R. 1994. Examination of atmospheric bioaerosol particles with radii >0.2 μm. *J. Aerosol. Sci.* 25:1605–13

Maynard AD. 1995. The application of electron energy-loss spectroscopy to the analysis of ultrafine aerosol particles. *J. Aerosol. Sci.* 26:757–77

Middlebrook AM, Murphy DM, Thomson DS. 1998. Observations of organic material in individual marine particles at Cape Grim during the First Aerosol Characterization Experiment (ACE 1). *J. Geophys. Res.* 103:16475–83

Mishchenko MI, Hovenier JW, Travis LD, eds. 2000. *Light Scattering by Nonspherical Particles: Theory, Measurements, and Applications*. London: Academic. 640 pp.

Möhler O, DeMott PJ, Vali G, Levin Z. 2007. Microbiology and atmospheric processes: the role of biological particles in cloud physics. *Biogeosciences* 4:1059–71

Morris CE, Sands DC, Bardin M, Jaenicke R, Vogel B, et al. 2008. Microbiology and atmospheric processes: an upcoming era of research on bio-meteorology. *Biogeosci. Discuss.* 5:191–212

Murphy DM. 2005. Something in the air. *Science* 307:1888–90

Murphy DM, Anderson JR, Quinn PK, Mclnnes LM, Brechtel FJ, et al. 1998. Influence of sea-salt on aerosol radiative properties in the Southern Ocean marine boundary layer. *Nature* 392:62–65

Murphy DM, Cziczo DJ, Froyd KD, Hudson PK, Matthew BM, et al. 2006. Single-particle mass spectrometry of tropospheric aerosol particles. *J. Geophys. Res.* 111:D23S32, doi:10.1029/2006JD007340

Niemi JV, Saarikoski S, Tervahattu H, Mäkelä T, Hillamo R, et al. 2006. Changes in background aerosol composition in Finland during polluted and clean periods studied by TEM/EDX individual particle analysis. *Atmos. Chem. Phys.* 6:5049–66

Niemi JV, Tervahattu H, Vehkamäki H, Kulmala M, Koskentalo T, et al. 2004. Characterization and source identification of a fine particle episode in Finland. *Atmos. Environ.* 38:5003–12

Niimura N, Okada K, Fan X-B, Kai K, Arao K, et al. 1998. Formation of Asian dust-storm particles mixed internally with sea salt in the atmosphere. *J. Meteorol. Soc. Jpn.* 76:275–88

O'Dowd CD, Facchini MC, Cavalli F, Ceburnis D, Mircea M, et al. 2004. Biogenically driven organic contribution to marine aerosol. *Nature* 431:676–80

O'Dowd CD, Smith MH, Consterdine IE, Lowe JA. 1997. Marine aerosol, sea-salt, and the marine sulphur cycle: a short review. *Atmos. Environ.* 31:73–80

Okada K, Ikegami M, Zaizen Y, Tsutsumi Y, Makino Y, et al. 2005. Soot particles in the free troposphere over Australia. *Atmos. Environ.* 39:5079–89

Okada K, Kai K. 2004. Atmospheric mineral particles collected at Qira in the Taklamakan Desert, China. *Atmos. Environ.* 38:6927–35

Palotas AB, Rainey LC, Feldermann CJ, Sarofim AF, Vander Sande JB. 1996. Soot morphology: an application of image analysis in high-resolution transmission electron microscopy. *Microsc. Res. Tech.* 33:266–78

Pant A, Fok A, Parsons MT, Mak J, Bertram AK. 2004. Deliquescence and crystallization of ammonium sulfate–glutaric acid and sodium chloride–glutaric acid particles. *Geophys. Res. Lett.* 31:L12111, doi:10.1029/2004GL020025

Pósfai M, Anderson JR, Buseck PR, Sievering H. 1995. Compositional variations of sea-salt-mode aerosol particles from the North Atlantic. *J. Geophys. Res.* 100(D11):23063–74

Pósfai M, Anderson JR, Buseck PR, Sievering H. 1999. Soot and sulfate aerosol particles in the remote marine troposphere. *J. Geophys. Res.* 104:21685–93

Pósfai M, Gelencsér A, Simonics R, Arató K, Li J, et al. 2004. Atmospheric tar balls: particles from biomass and biofuel burning. *J. Geophys. Res.* 109:D06213, doi:10.1029/2003JD004169

Pósfai M, Li J, Anderson JR, Buseck PR. 2003a. Aerosol bacteria over the Southern Ocean during ACE-1. *Atmos. Res.* 66:231–40

Pósfai M, Molnár A. 2000. Aerosol particles in the troposphere: a mineralogical introduction. In *Environmental Mineralogy*, ed. DJ Vaughan, RA Wogelius, pp. 197–252. Budapest: Eötvös Univ. Press

Pósfai M, Simonics R, Li J, Hobbs PV, Buseck PR. 2003b. Individual aerosol particles from biomass burning in southern Africa: 1. Compositions and size distributions of carbonaceous particles. *J. Geophys. Res.* 108:8483, doi:10.1029/2002JD002291

Pósfai M, Xu H, Anderson JR, Buseck PR. 1998. Wet and dry sizes of atmospheric aerosol particles: an AFM-TEM study. *Geophys. Res. Lett.* 25:1907–10

Post JE, Buseck PR. 1984. Characterization of individual particles in the Phoenix urban aerosol using electron-beam instruments. *Environ. Sci. Technol.* 18:35–42

Prospero JM. 1999. Long-range transport of mineral dust in the global atmosphere: impact of African dust on the environment of the southeastern United States. *Proc. Natl. Acad. Sci. USA* 96:3396–403

Ramanathan V, Carmichael G. 2008. Global and regional climate changes due to black carbon. *Nat. Geosci.* 1:221–27

Ramanathan V, Ramana MV, Roberts G, Kim D, Corrigan C, et al. 2007. Warming trends in Asia amplified by brown cloud solar absorption. *Nature* 448:575–78

Ramirez-Aguilar KA, Lehmpuhl DW, Michel AE, Birks JW, Rowlen KL. 1999. Atomic force microscopy for the analysis of environmental particles. *Ultramicroscopy* 77:187–94

Reid JS, Koppmann R, Eck TF, Eleuterio DP. 2005. A review of biomass burning emissions part II: intensive physical properties of biomass burning particles. *Atmos. Chem. Phys.* 5:799–825

Russell LM, Maria SF, Myneni SCB. 2002. Mapping organic coatings on atmospheric particles. *Geophys. Res. Lett.* 29(16):1779, doi:10.1029/2002GL014874

Sattler B, Puxbaum H, Psenner R. 2001. Bacterial growth in supercooled cloud droplets. *Geophys. Res. Lett.* 28:243–46

Schnaiter M, Linke C, Möhler O, Naumann K-H, Saathoff H, et al. 2005. Absorption amplification of black carbon internally mixed with secondary organic aerosol. *J. Geophys. Res.* 110:D19204, doi:10.1029/2005JD006046

Schwarz JP, Spackman JR, Fahey DW, Gao RS, Lohmann U, et al. 2008. Coatings and their enhancement of black carbon light absorption in the tropical atmosphere. *J. Geophys. Res.* 113:D03203, doi:10.1029/2007JD009042

Seinfeld JH, Pandis SN. 2006. *Atmospheric Chemistry and Physics: From Air Pollution to Climate Change*. New York: Wiley. 1232 pp. 2nd ed.

Semeniuk TA, Wise ME, Martin ST, Russell LM, Buseck PR. 2007a. Hygroscopic behavior of aerosol particles from biomass fires using environmental transmission electron microscopy. *J. Atmos. Chem.* 56:259–73

Semeniuk TA, Wise ME, Martin ST, Russell LM, Buseck PR. 2007b. Water uptake characteristics of individual atmospheric particles having coatings. *Atmos. Environ.* 41:6225–35

Shi Z, Zhang D, Hayashi M, Ogata H, Ji H, Fujiie W. 2008. Influences of sulfate and nitrate on the hygroscopic behaviour of coarse dust particles. *Atmos. Environ.* 42:822–27

Smekens A, Godoi RHM, Vervoort M, Van Espen P, Potgieter-Vermaak SS, Van Grieken R. 2007. Characterization of individual soot aggregates from different sources using image analysis. *J. Atmos. Chem.* 56:211–23

Smith JN, Dunn MJ, VanReken TM, Iida K, Stolzenburg MR, et al. 2008. Chemical composition of atmospheric nanoparticles formed from nucleation in Tecamac, Mexico: evidence for an important role for organic species in nanoparticle growth. *Geophys. Res. Lett.* 35:L04808, doi:10.1029/2007GL032523

Sobanska S, Coeur C, Maenhaut W, Adams F. 2003. SEM-EDX characterisation of trophospheric aerosols in the Negev desert (Israel). *J. Atmos. Chem.* 44:299–322

Sorensen CM. 2001. Light scattering by fractal aggregates: a review. *Aerosol Sci. Technol.* 35:648–87

Sun J, Ariya PA. 2006. Atmospheric organic and bio-aerosols as cloud condensation nuclei (CCN): a review. *Atmos. Environ.* 40:795–820

Sze S-K, Siddique N, Sloan JJ, Escribano R. 2001. Raman spectroscopic characterization of carbonaceous aerosols. *Atmos. Environ.* 35:561–68

Takahama S, Gilardoni S, Russell LM, Kilcoyne ALD. 2007. Classification of multiple types of organic carbon composition in atmospheric particles by scanning transmission X-ray microscopy analysis. *Atmos. Environ.* 41:9435–51

Targino AC, Krejci R, Noone KJ, Glantz P. 2006. Single particle analysis of ice crystal residuals observed in orographic wave clouds over Scandinavia during INTACC experiment. *Atmos. Chem. Phys.* 6:1977–90

Tivanski AV, Hopkins RJ, Tyliszczak T, Gilles MK. 2007. Oxygenated interface on biomass burn tar balls determined by single particle scanning transmission X-ray microscopy. *J. Phys. Chem. A* 111:5448–58

Travis DJ, Carleton AM, Lauritsen RG. 2002. Contrails reduce daily temperature range. *Nature* 418:601

Trochkine D, Iwasaka Y, Matsuki A, Yamada M, Kim Y-S, et al. 2003. Mineral aerosol particles collected in Dunhuang, China, and their comparison with chemically modified particles collected over Japan. *J. Geophys. Res.* 108(D23):8642, doi:10.1029/2002JD003268

Tsigaridis K, Kanakidou M. 2007. Secondary organic aerosol importance in the future atmosphere. *Atmos. Environ.* 41:4682–92

Twohy CH, Anderson JR, Crozier PA. 2005. Nitrogenated organic aerosols as cloud condensation nuclei. *Geophys. Res. Lett.* 32:L19805, doi:10.1029/2005GL023605

Twohy CH, Gandrud BW. 1998. Electron microscope analysis of residual particles from aircraft contrails. *Geophys. Res. Lett.* 25:1359–62

Twomey SA. 1977. The influence of pollution on the shortwave albedo of clouds. *J. Atmos. Sci.* 34:1149–52

Vali G. 1985. Atmospheric ice nucleation—a review. *J. Rech. Atmos.* 19:105–15

van Poppel LH, Friedrich H, Spinsby J, Chung SH, Seinfeld JH, Buseck PR. 2005. Electron tomography of nanoparticle clusters: implications for atmospheric lifetimes and radiative forcing of soot. *Geophys. Res. Lett.* 32:L24811, doi:10.1029/2005GL024461

Wang J, Jacob DJ, Martin ST. 2008. Sensitivity of sulfate direct climate forcing to the hysteresis of particle phase transitions. *J. Geophys. Res.* 113:D11207, doi:10.1029/2007JD009368

Wentzel M, Gorzawski H, Naumann KH, Saathoff H, Weinbruch S. 2003. Transmission electron microscopical and aerosol dynamical characterization of soot aerosols. *J. Aerosol. Sci.* 34:1347–70

Wild M, Ohmura A, Makowski K. 2007. Impact of global dimming and brightening on global warming. *Geophys. Res. Lett.* 34:L04702, doi:10.1029/2006GL028031

Winiwarter W, Bauer H, Caseiro A, Puxbaum H. 2009. Quantifying emissions of primary biological aerosol particle mass in Europe. *Atmos. Environ.* 43(7):1403–9

Winterholler B, Hoppe P, Huth J, Foley S, Andreae MO. 2008. Sulfur isotope analyses of individual aerosol particles in the urban aerosol at a central European site (Mainz, Germany). *Atmos. Chem. Phys. Discuss.* 8:9347–404

Wise ME, Biskos G, Martin ST, Russell LM, Buseck PR. 2005. Phase transitions of single salt particles studied using a transmission electron microscope with an environmental cell. *Aerosol Sci. Technol.* 39:849–56

Wise ME, Semeniuk TA, Bruintjes R, Martin ST, Russell LM, Buseck PR. 2007. Hygroscopic behavior of NaCl-bearing natural aerosol particles using environmental transmission electron microscopy. *J. Geophys. Res.* 112:D10224, doi:10.1029/2006JD007678

Wurzler S, Reisin TG, Levin Z. 2000. Modification of mineral dust particles by cloud processing and subsequent effects on drop size distributions. *J. Geophys. Res.* 105:4501–12

Yu H, Kaufman YJ, Chin M, Feingold G, Remer LA, et al. 2006. A review of measurement-based assessments of the aerosol direct radiative effect and forcing. *Atmos. Chem. Phys.* 6:613–66

Zangmeister CD, Pemberton JE. 2000. Raman spectroscopy and atomic force microscopy of the reaction of sulfuric acid with sodium chloride. *J. Am. Chem. Soc.* 122:12289–96

Zhang R, Suh I, Zhao J, Zhang D, Fortner EC, et al. 2004. Atmospheric new particle formation enhanced by organic acids. *Science* 304:1487–90

Zimmermann F, Ebert M, Worringen A, Schütz L, Weinbruch S. 2007. Environmental scanning electron microscopy (ESEM) as a new technique to determine the ice nucleation capability of individual atmospheric aerosol particles. *Atmos. Environ.* 41:8219–27

Annual Review
of Earth and
Planetary Sciences

Volume 38, 2010

Contents

Indexes

Errata

An online log of corrections to *Annual Review of Earth and Planetary Sciences* articles may be found at http://earth.annualreviews.org